Dynamical equivalence between Kuramoto models with first- and higher-order coupling

View Online   Export Citation   CrossMark

Robin Delabays[1,2] (ID)

AFFILIATIONS

[1] School of Engineering, University of Applied Sciences of Western Switzerland, CH-1950 Sion, Switzerland
[2] Institut für Automatik, ETH Zürich, CH-8092 Zürich, Switzerland

ABSTRACT

The Kuramoto model with high-order coupling has recently attracted some attention in the field of coupled oscillators in order, for instance, to describe clustering phenomena in sets of coupled agents. Instead of considering interactions given directly by the sine of oscillators' angle differences, the interaction is given by the sum of sines of integer multiples of these angle differences. This can be interpreted as a Fourier decomposition of a general 2π-periodic interaction function. We show that in the case where only one multiple of the angle differences is considered, which we refer to as the "Kuramoto model with simple qth-order coupling," the system is dynamically equivalent to the original Kuramoto model. In other words, any property of the Kuramoto model with simple higher-order coupling can be recovered from the standard Kuramoto model.

Published under license by AIP Publishing. https://doi.org/10.1063/1.5118941

Along the last few decades, the Kuramoto model has attracted a lot of interest in the field of synchronization of coupled oscillators. Its simple formulation and the variety of synchronization phenomena that it describes make it a good candidate to investigate such phenomena both numerically and analytically. The sinusoidal interaction in the Kuramoto model can be seen as the first order of the Fourier decomposition of a general coupling function. It is then natural to extend the coupling to higher orders, such that the dynamics depend on the sines of multiples of the angle differences. In this paper, we show that considering only the angle difference or a unique integer multiple of it in the sinusoidal coupling is qualitatively equivalent.

I. INTRODUCTION

In the context of synchronization of coupled dynamical systems, the Kuramoto model[1,2] has drawn much attention within the last few decades.[3–5] Synchrony is observed in many real systems, ranging from the brain's oscillatory pacemaker cells establishing the circadian rhythm[6] to synchronous machines connected to the high-voltage AC electrical grid.[7,8] This popularity brought the topic to a point where the remaining open questions are both hard and poorly rewarding to answer. To describe more realistic systems, some generalized versions of the Kuramoto model have been considered, for instance, meshed interaction graphs, higher-order dynamics,[8] or

directed interactions.[9,10] One of these generalizations is to consider higher-order couplings.[11–18] While the Kuramoto model is defined as

$$\dot{\theta}_i = \omega_i - \frac{K}{n} \sum_{j=1}^{n} \sin(\theta_i - \theta_j) \qquad (1.1)$$

for $i \in \{1, \dots, n\}$, where $\theta_i \in \mathbb{R}$ is the ith oscillator's angle, $\omega_i \in \mathbb{R}$ is its natural frequency, and $K > 0$ is the coupling strength, the Kuramoto model with qth-order coupling, for $q \in \mathbb{Z}_{>0}$, is defined as

$$\dot{\theta}_i = \omega_i - \sum_{j=1}^{n} \sum_{\ell=1}^{q} \frac{K_\ell}{n} \sin\left[\ell \cdot (\theta_i - \theta_j)\right] \qquad (1.2)$$

for $i \in \{1, \dots, n\}$. The sum over ℓ can be seen as a truncated Fourier decomposition of a general 2π-periodic coupling function.

To this day, most of the works about this version of the model have been limited to second-order couplings ($K_{1,2} \neq 0$), which already exhibits behaviors significantly different from the original Kuramoto model.[14–17] While most descriptions of the synchronous states of this model, for $q = 2$ and large n, have been performed numerically,[15,16] an analytical approach, based on a self-consistency equation for the order parameters of the system, is given in Ref. 14. The Kuramoto model with qth-order coupling has been used to describe clustering phenomena in systems of coupled synchronized oscillators. Clustered synchronous states of some particular

versions of the Kuramoto model with second-order coupling and their dynamics are described in Refs. 11 and 12.

When one of the coupling orders largely dominates the others, a simplifying assumption is to consider the case where $K_\ell = 0$ for all $\ell \neq q$, which we refer to as the Kuramoto model with simple qth-order coupling.[13,18] In this case, Eq. (1.2) reduces to

$$\dot{\theta}_i = \omega_i - \frac{K}{n} \sum_{j=1}^{n} \sin\left[q \cdot (\theta_i - \theta_j)\right] \qquad (1.3)$$

for $i \in \{1, \ldots, n\}$, which is the dynamical system considered in this paper. Note that the Kuramoto model, Eq. (1.1), can be seen as the Kuramoto model with simple first-order coupling. An analytical description of the transient dynamics of Eq. (1.3) and its synchronous clustered states is given in Ref. 13.

In this paper, we show that the dynamical systems described by Eqs. (1.1) and (1.3) are qualitatively equivalent, in the sense that both have the same dynamical properties (fixed points, linear stability, basin stability, order parameter) up to a projection from the state space to itself. Doing so, we make rigorous the claim below Eq. (3) in Ref. 15 that "In the case with $K_1 = 0$ (or $K_2 = 0$), the model is reduced to the original [Kuramoto model]...." It also explains the striking similarity between Fig. 2 in Ref. 18 (the Kuramoto model with simple second-order coupling) and Fig. 2 in Ref. 19 (the Kuramoto model with simple first-order coupling). In Sec. II, we see that a direct relation can be drawn between the two models, allowing to translate any property of one model to the other. Therefore, a thorough investigation of the Kuramoto model with simple qth-order coupling is not needed, as any of its properties can be derived from properties of the original Kuramoto model. A selection of such properties and some implications for potential applications are detailed in Sec. III.

Remark.   *In Eq. (1.3), we consider all-to-all coupling, and we will do so for the whole paper for the sake of readability. Nevertheless, our results can be straightforwardly extended to any coupling graph. We comment on this at the end of Sec. III.*

II. DYNAMICAL EQUIVALENCE

The Kuramoto model is usually considered a dynamical system on the torus $\mathbb{T}^n$. We consider the variables θ_i as elements of $\mathbb{S}^1$, which we parametrize as $[0, 2\pi)$ with periodic boundary conditions. We show now that the following two dynamical systems:

$$\dot{\theta}_i = q\omega_i - \frac{qK}{n} \sum_{j=1}^{n} \sin\left(\theta_i - \theta_j\right), \qquad (2.1)$$

$$\dot{\theta}_i = \omega_i - \frac{K}{n} \sum_{j=1}^{n} \sin\left[q \cdot (\theta_i - \theta_j)\right], \qquad (2.2)$$

describe the same dynamics, up to rescaling the variables θ_i by a factor q. The rescaling is performed by the covering map from $\mathbb{T}^n$ to itself, which we define parametrically as

$$\pi_q : \mathbb{T}^n \longrightarrow \mathbb{T}^n,$$
$$(\theta_1, \ldots, \theta_n) \longmapsto (q\theta_1, \ldots, q\theta_n) \mod 2\pi, \qquad (2.3)$$

where the modulo is applied elementwise.

More formally, we show below that π_q sends any solution of Eq. (2.2) to a solution of Eq. (2.1) and that any lift of a solution of Eq. (2.1) through π_q is a solution of Eq. (2.2). As π_q is a smooth covering map, all properties of a solution of Eq. (2.2) are preserved in its projection [and similarly for the lift of a solution of Eq. (2.1)]. This is what we mean by "dynamical equivalence."

A. Projecting

Let $\Theta_{\psi^*} : \mathbb{R} \to \mathbb{T}^n$ be the solution of Eq. (2.2) with initial conditions ψ^*. We verify that the projection $\pi_q \Theta_{\psi^*}(t)$ solves Eq. (2.1),

$$\frac{\mathrm{d}}{\mathrm{d}t} \pi_q \Theta_{\psi^*} = q\omega_i - \frac{qK}{n} \sum_{j=1}^{n} \sin\left[q\left(\Theta_{\psi^*,i} - \Theta_{\psi^*,j}\right)\right] \qquad (2.4)$$

$$= q\omega_i - \frac{qK}{n} \sum_{j=1}^{n} \sin\left(\pi_q \Theta_{\psi^*,i} - \pi_q \Theta_{\psi^*,j}\right), \qquad (2.5)$$

with initial conditions $\pi_q \Theta_{\psi^*}(0) = q\psi^*$.

B. Lifting up

The other way is a bit more intricate because there are multiple preimages through π_q^{-1} for each element of $\mathbb{T}^n$. Let $\Phi_{\eta^*} : \mathbb{R} \to \mathbb{T}^n$ be the solution of Eq. (2.1) with initial conditions $\eta^* \in \mathbb{T}^n$. The preimage $\pi_q^{-1} \eta^*$ is a set of q^n points, one of them being $q^{-1}\eta^* \in [0, 2\pi/q)^n \subset \mathbb{T}^n$, whose ith component is η_i/q. The other $q^n - 1$ can be constructed as

$$q^{-1}\eta^* + \frac{2\pi}{q}\rho, \qquad (2.6)$$

with $\rho \in \{0, 1, \ldots, q-1\}^n$. Each one of these points can be chosen as a starting point for the lifting.

Now, whichever element $\psi^* \in \pi_q^{-1}\eta^*$ we choose as starting point for the lifting, there is a unique smooth lifting $\pi_q^{-1}\Phi_{\eta^*}(t)$ of the trajectory $\Phi_{\eta^*}(t)$ satisfying the following two properties:

(i) $\pi_q^{-1}\Phi_{\eta^*}(0) = \psi^*$,

(ii) $\pi_q \left[\pi_q^{-1}\Phi_{\eta^*}(t)\right] = \Phi_{\eta^*}(t)$, for all $t \in \mathbb{R}$.

The time derivative of the ith component of this lifting is

$$\frac{\mathrm{d}}{\mathrm{d}t}\left(\pi_q^{-1}\Phi_{\eta^*}\right)_i = q^{-1}\dot{\Phi}_{\eta^*,i} \qquad (2.7)$$

$$= q^{-1}\left[q\omega_i - \frac{qK}{n}\sum_{j=1}^{n}\sin\left(\Phi_{\eta^*,i} - \Phi_{\eta^*,j}\right)\right] \qquad (2.8)$$

$$= \omega_i - \frac{K}{n}\sum_{j=1}^{n}\sin\left[q\left(\pi_q^{-1}\Phi_{\eta^*,i} - \pi_q^{-1}\Phi_{\eta^*,j}\right)\right]. \qquad (2.9)$$

The lifting then solves Eq. (2.2) with initial conditions ψ^*, and this is true independently of the choice of representative $\psi^* \in \pi_q^{-1}\eta^*$. The preimage, by π_q^{-1}, of a solution Φ_{η^*} of Eq. (2.1) is then a set of solutions of Eq. (2.2) differing from one another by a shift $2\pi\rho/q$, with $\rho \in \{0, 1, \ldots, q-1\}^n$.

C. Dynamical equivalence

It is now clear that

$$\pi_q\left(\pi_q^{-1}\Phi_{\boldsymbol{\eta}^*}\right) = \Phi_{\boldsymbol{\eta}^*}, \tag{2.10}$$

and the unique smooth lifting of $\pi_q\Theta_{\boldsymbol{\psi}^*}$ such that $\pi_q^{-1}\left(\pi_q\Theta_{\boldsymbol{\psi}^*}\right)(0) = \boldsymbol{\psi}^*$ is exactly

$$\pi_q^{-1}\left(\pi_q\Theta_{\boldsymbol{\psi}^*}\right) = \Theta_{\boldsymbol{\psi}^*}. \tag{2.11}$$

Properties of the solutions are then preserved by the projection π_q as well as by its corresponding lifting. We verify this for some dynamical properties in Sec. III.

III. CONSEQUENCES ON CLUSTERING

Now that we established the dynamical equivalence between the Kuramoto model with simple first- and higher-order coupling, we review some results known for the original Kuramoto model and translate them in the Kuramoto model with qth-order coupling, in order to derive some results about clustering in the latter.

A. Fixed points

A given fixed point of the original Kuramoto model corresponds to q^n fixed points of the Kuramoto model with qth-order coupling. Each of these fixed points differs by a shift $2\pi\boldsymbol{\rho}/q$, with $\boldsymbol{\rho} \in \{0, 1, \ldots, q-1\}^n$. When the natural frequencies are small ($\omega_i \ll K/n$), the synchronous state $\boldsymbol{\theta}^* \in [0, 2\pi)^n$ of Eq. (2.1) is such that all angles are close to each other. For any $\boldsymbol{\rho} \in \{0, 1, \ldots, q-1\}^n$, the point $2\pi\boldsymbol{\rho}/q \in [0, 2\pi)^n$ is a synchronous state for Eq. (2.2). The integer vector $\boldsymbol{\rho}$ describes the "clustering pattern" of the corresponding synchronous state. If $\rho_i = \rho_j$, oscillators i and j are close to each other (at least for rather small natural frequencies) and approximately $2\pi/q$ apart from an oscillator k such that $\rho_k = \rho_i \pm 1$. Then, each oscillators with the same value in $\boldsymbol{\rho}$ form a cluster. The number of

different values in $\boldsymbol{\rho}$ gives the total number of clusters in the synchronous state under consideration. From the point of view of the dynamics, however, the clustering pattern has no effect. The $2\pi/q$ shifts introduced by the vector $\boldsymbol{\rho}$ leave Eq. (2.2) unchanged. The only information that is lost between the qth- and first-order coupling Kuramoto models is the clustering pattern. However, this is only a combinatorial problem that can be addressed independently of dynamical considerations. In Fig. 1, for instance, each color corresponds to a different clustering. At the end of the trajectory, the orange line has five oscillators in one cluster ($\{1, 2, 3, 4, 6\}$), with angles in $[0, \pi)$ and oscillator 5 forming a cluster by itself, with its angle in $[\pi, 2\pi)$. Similarly, for the green line, oscillators 1 and 3 are in one cluster with angles in $[0, \pi)$ and the others are in the cluster with angles in $[\pi, 2\pi)$.

B. Linear stability

One can verify that the linear stability of Eq. (2.2) at a fixed point $\boldsymbol{\theta}^*$ is identical to the linear stability of Eq. (2.1) at $\pi_q\boldsymbol{\theta}^*$. More precisely, the Jacobian matrices $\mathcal{J}_q(\boldsymbol{\theta}^*)$ of Eq. (2.2) at $\boldsymbol{\theta}^*$ and $\mathcal{J}_1(\pi_q\boldsymbol{\theta}^*)$ of Eq. (2.1) at $\pi_q\boldsymbol{\theta}^*$ are equal. Thus, for a given distribution of natural frequencies, all clustered states have the same linear stability properties.

C. Order parameter

The order parameter r_1 is a quantity describing the level of coherence between oscillators' angles in the Kuramoto model. It has been a major ingredient to analyze synchronization in this model.[1,20–22] To take clustering into account, in the Kuramoto model with higher-order coupling, it has been generalized[13] to the qth order parameter,

$$r_q(\boldsymbol{\theta}) := \frac{1}{n}\left|\sum_{j=1}^{n} e^{iq\theta_j}\right|. \tag{3.1}$$
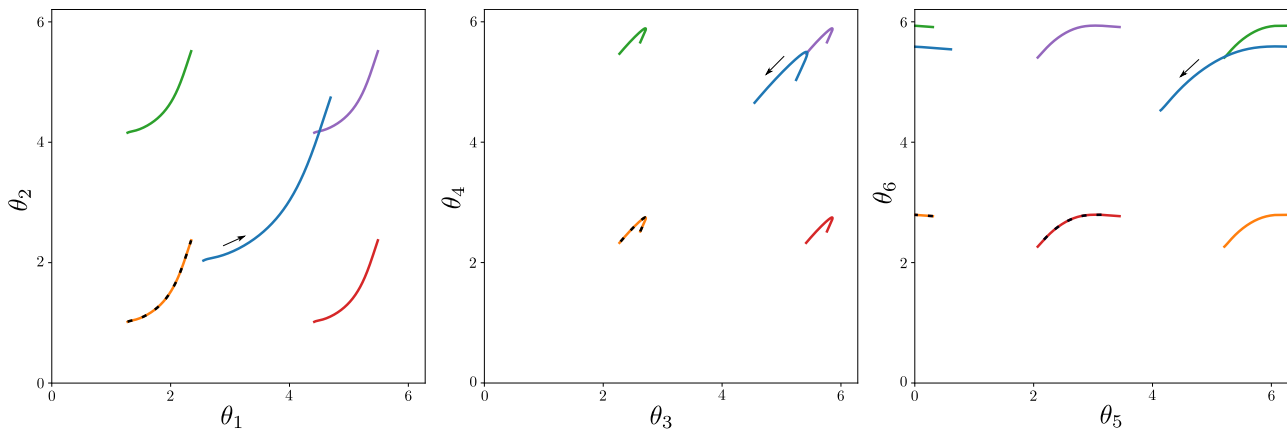

FIG. 1. Example of the trajectories of the dynamical systems Eq. (2.1) (blue) and Eq. (2.2) (orange, green, red, and purple), with $n = 6$ and $q = 2$. Boundary conditions are periodic. Initial conditions were, respectively, $\boldsymbol{\psi}^* \in [0, 2\pi/q)^n$ (orange, taken randomly), $\boldsymbol{\psi}^* + (\pi, 0, \pi, 0, \pi, 0)$ (red), $\boldsymbol{\psi}^* + (0, \pi, 0, \pi, 0, \pi)$ (green), $\boldsymbol{\psi}^* + (\pi, \pi, \pi, \pi, \pi, \pi)$ (purple), and $q\boldsymbol{\psi}^*$ (blue). The black dashed line is obtained by dividing all angles of the solution of Eq. (2.1) (blue) by q. The arrow shows the direction of the time evolution. The solutions of Eq. (2.2) are simply translations of each other, and the solution of (2.1) is a homogeneous dilatation of factor q of the others.

It directly translates from the Kuramoto model with simple qth-order coupling to its equivalent Kuramoto model with first-order coupling. Namely, the order parameter $r_q(\theta^*)$ is equal to $r_1(\pi_q\theta^*)$. A large qth order parameter r_q indicates that the current state of Eq. (2.2) is clustered but does not give any information about the clustering pattern because it is blind to any angle shift of $2\pi/q$. The order parameter r_q takes the same value $r = r_1(\psi^*)$ for each element of the preimage $\pi_q^{-1}\psi^*$.

More generally, $r_p \approx 1$ for $1 \leq p \leq q$ indicates that the system is clustered in p equidistance clusters. Furthermore, if $r_p \approx 1$, it implies that $r_{kp} \approx 1$ for any $k \in \mathbb{N}$. Looking at all the order parameters with $1 \leq p \leq q$ can give more information about the clustering pattern. For instance, in the special case where $q = 2$, if $r_2 = 1$, then one can verify that the number of oscillators in each cluster n_1 and n_2, respectively, are given by

$$n_1 = \frac{(1+r_1)n}{2}, \quad n_2 = \frac{(1-r_1)n}{2}. \tag{3.2}$$

In more general cases, however, it is not possible, as far as we can tell, to determine the number of oscillators in each cluster only based on the order parameters.

D. Synchronization

It is known[23] for the Kuramoto model, Eq. (2.1), that if the coupling is sufficiently large to grant the existence of a synchronous state $[K > \max_{i,j}(\omega_i - \omega_j)]$, then there exists a value $\gamma_{\max} \in (\pi/2, \pi]$ such that the system synchronizes if all initial angles are in an arc of length at most $\gamma_{\max}$. In the Kuramoto model with simple qth-order coupling, this translates as follows. First, for the same value of K, the system synchronizes to the single cluster fixed point if all initial angles are in an arc of length $\gamma_{\max}/q$. Second, if the initial conditions ψ^* are such that all angles of $\psi^* - 2\pi\rho^*/q$ are contained in an arc of length $\gamma_{\max}/q$, then the system synchronizes to the state with clusters given by $\rho^* \in \{0, 1, \ldots, q-1\}^n$.

E. Basins of attraction

By equivalence of the dynamics, the basin of attraction of fixed point θ^* of Eq. (2.2) is a copy of the basin of attraction of the fixed point $\pi_q\theta^*$ of Eq. (2.1), rescaled by a factor q^{-1}. Namely, its volume is q^{-n} times the volume of the basin of attraction of $\pi_q\theta^*$. We illustrate this in Fig. 2, where we show the basins of attraction for the systems (2.1) (left panel) and (2.2) (right panel).

F. Basin escape

Suppose we introduce an additive noise in Eq. (2.2) to account for unpredictable perturbation of the environment. This will eventually lead our system to jump from a synchronous state to another.[24,25] For the Kuramoto model, Eq. (2.1), such jumps bring the system from a synchronous state to a translate of itself, where some angles slip and accumulate integer multiples of 2π. Lifting up such a trajectory to the Kuramoto model with simple qth-order coupling, the jumps then occur between the basins of attraction of different clustered states, where some angles accumulate an integer multiple of $2\pi/q$. Additive noise in Eq. (2.2) is then a possible mechanism for cluster formation.
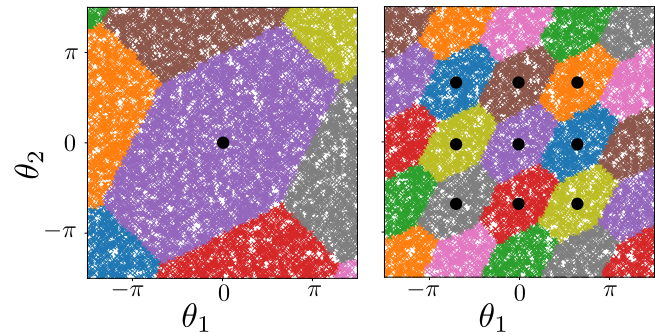

FIG. 2. Basins of attraction of various synchronous states of Eq. (2.1) (left panel) and Eq. (2.2) (right panel) with $n = 3$, $q = 3$, and identical natural frequencies ($\omega_i \equiv 0$). The angle θ_3 was fixed at 0, to remove the degree of freedom corresponding to the constant angle shift. Each figure is composed of 10 000 random initial conditions, and the color of each cross depends on the state to which it synchronizes. For the Kuramoto model, Eq. (2.1), all initial conditions converge to the same synchronous state (black dot, left panel), the colors only indicate if some angles accumulated a multiple of 2π due to the dynamics. For the Kuramoto model with simple qth-order coupling, Eq. (2.2), there are nine different synchronous states (black dots, right panel), with different clustering patterns, and the other basins correspond to translations of these nine basins. This illustrates that the basins of Eq. (2.2) are a copy of those of Eq. (2.1) rescaled by a factor $1/3$.

If the noise has sufficiently small amplitude, the system remains for a long time in a neighborhood of a synchronous state, until the noise generates a sequence of perturbations that make it jump to another synchronous state. As pointed out by previous research on the Kuramoto model,[24,26] the expected time between two jumps is exponential in (i) the inverse of the natural frequencies' distribution width and (ii) the potential difference between the initial synchronous states and the closest 1-saddle. It can also be related to (iii) the distance (in the state space) between the stable synchronous state and the closest 1-saddle.[25] By the equivalence derived in Sec. II, the expected time between jumps from a clustering pattern to another then follows the same exponential dependence (i)–(iii).

The equivalence is clearly seen in Fig. 3, where the angle trajectories in the two systems seem to be rescaled copies of each other, while they are obtained by two different simulations. The difference being that in the original Kuramoto model, the system jumps from the unique synchronous state to itself, by periodicity of the phase space, while in the Kuramoto model with qth-order coupling, the jumps occur between different clustered states.

G. Information storage

It has been acknowledged[27,28] that the dynamics of some real-world systems can be described rather accurately by Eq. (2.2). In particular, it was proposed that such systems could be used as information storage,[13,29] where the value of each lower order parameter is a piece of information. Reference 13 defines a forcing that allows determining the clustered state to which the system synchronizes and thus to control the value of r_p for $1 \leq p < q$. In this scope, the dynamical equivalence shown in Sec. II indicates that the stability properties of the system do not depend on its states. This is of major importance
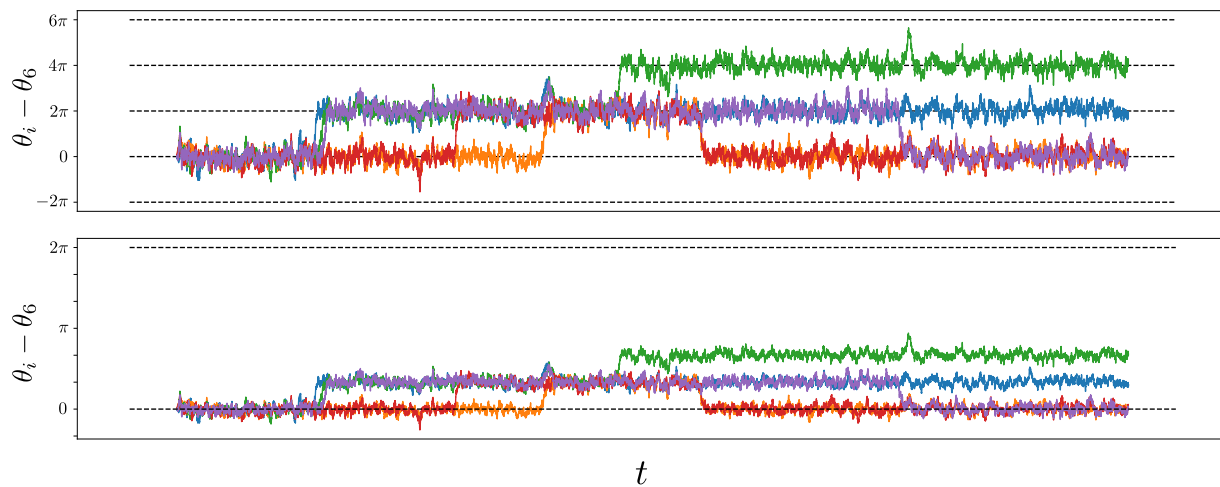
FIG. 3. Time evolution of the angles in the Kuramoto model (top panel) and the Kuramoto model with simple 6th-order coupling (bottom panel) with $n = 6$, both subject to additive white noise. Initial conditions are $(0, \ldots, 0)$ for both systems, natural frequencies are identically zero, and the coupling is $K_1 = 1$ and $K_6 = 1/6$, respectively. The noise sequences are the same, with amplitude divided by 6 for the Kuramoto model with 6th-order coupling. The black dashed lines indicate the multiple of 2π, i.e., the limits of the periodic boundary conditions. After each jump in the Kuramoto model, the system converges back to its initial conditions, whereas with 6th-order coupling, the Kuramoto model converges to a clustered state, even if the trajectories are qualitatively the same, this is only due to the different coupling functions.

for such an application as it guarantees that the reliability of the storage system does not depend on the information it contains, which would render such an application much more complicated.

H. Generalization

More generally, instead of nonoriented, homogeneous, all-to-all couplings, our argument can be straightforwardly extended to the Kuramoto model with interactions given by any graph, weighted or not, directed or not. Our argument also shows dynamical equivalence between the following two, more general versions of the Kuramoto model with higher-order coupling:

$$\dot{\theta}_i = \omega_i - \sum_{j=1}^{n} \sum_{\ell=1}^{q} \frac{K_\ell}{n} \sin\left[\ell p \cdot (\theta_i - \theta_j)\right], \qquad (3.3)$$

$$\dot{\theta}_i = p\omega_i - \sum_{j=1}^{n} \sum_{\ell=1}^{q} \frac{pK_\ell}{n} \sin\left[\ell \cdot (\theta_i - \theta_j)\right] \qquad (3.4)$$

for $i \in \{1, \ldots, n\}$ and $p \in \mathbb{Z}_{>0}$.

IV. CONCLUSION

The main consequence of the dynamical equivalence presented in this paper is that any property of the original Kuramoto model, Eq. (2.1), can be lifted to the Kuramoto model with simple qth-order coupling, Eq. (2.2). The only discrepancy is the multiplicity of the elements of the lifting from Eq. (2.2) to Eq. (2.1).

To summarize, we showed that the Kuramoto model with first-order coupling is dynamically equivalent to the Kuramoto model with simple qth-order coupling. As a matter of fact, any dynamical property of the latter can be derived from the corresponding property of the original Kuramoto model. The behavior of the Kuramoto model with higher-order coupling qualitatively changes only if at least two different coupling orders are considered. Clustering occurs in the Kuramoto model with simple qth-order coupling because of the choice of coupling function. However, the dynamics are blind to the clustering pattern as each synchronous state is dynamically equivalent.

To take into account clustered states whose characteristics (linear stability, basin shape, size, etc.) differ, other models should be used. Some promising examples are, for instance, the more general Kuramoto model with qth-order coupling [Eq. (1.2)] or some dynamical systems with bounded confidence.[30]

REFERENCES

[1] Y. Kuramoto, in *International Symposium on Mathematical Problems in Theoretical Physics*, Lecture Notes in Physics Vol. 39, edited by H. Araki (Springer, Berlin, 1975).
[2] Y. Kuramoto, Prog. Theor. Phys. Suppl. **79**, 223 (1984).
[3] S. H. Strogatz, Physica D **143**, 1 (2000).
[4] J. A. Acebrón, L. L. Bonilla, C. J. Pérez Vicente, F. Ritort, and R. Spigler, Rev. Mod. Phys. **77**, 137 (2005).
[5] F. Dörfler and F. Bullo, Automatica **50**, 1539 (2014).
[6] Z. Lu, K. Klein-Cardeña, S. Lee, T. M. Antonsen, M. Girvan, and E. Ott, Chaos **26**, 094811 (2016).
[7] A. R. Bergen and V. Vittal, *Power Systems Analysis* (Prentice Hall, 2000).
[8] F. Dörfler, M. Chertkov, and F. Bullo, Proc. Natl. Acad. Sci. U.S.A. **110**, 2005 (2013).
[9] J. G. Restrepo, E. Ott, and B. R. Hunt, Chaos **16**, 015107 (2006).

[10] R. Delabays, P. Jacquod, and F. Dörfler, SIAM J. Appl. Dyn. Syst. **18**, 458 (2019).

[11] D. Hansel, G. Mato, and C. Meunier, Phys. Rev. E **48**, 3470 (1993).

[12] H. Daido, Phys. Rev. Lett. **77**, 1406 (1996).

[13] P. S. Skardal, E. Ott, and J. G. Restrepo, Phys. Rev. E **84**, 036208 (2011).

[14] M. Komarov and A. Pikovsky, Phys. Rev. Lett. **111**, 204101 (2013).

[15] K. Li, S. Ma, H. Li, and J. Yang, Phys. Rev. E **89**, 032917 (2014).

[16] H. Wang, W. Han, and J. Yang, Phys. Rev. E **96**, 022202 (2017).

[17] S. Eydam and M. Wolfrum, Phys. Rev. E **96**, 052205 (2017).

[18] X. Li, J. Zhang, Y. Zou, and S. Guana, Chaos **29**, 043102 (2019).

[19] X. Li, T. Qiu, S. Boccaletti, I. Sendiña Nadal, Z. Liu, and S. Guan, New J. Phys. **21**, 053002 (2019).

[20] D. Aeyels and J. A. Rogge, Prog. Theor. Phys. **112**, 921 (2004).

[21] R. E. Mirollo and S. H. Strogatz, Physica D **205**, 249 (2005).

[22] M. Verwoerd and O. Mason, SIAM J. Appl. Dyn. Syst. **7**, 134 (2008).

[23] F. Dörfler and F. Bullo, in *Proceedings of the 2011 American Control Conference (ACC)* (IEEE, 2011), pp. 3239–3244.

[24] L. DeVille, Nonlinearity **25**, 1473 (2012).

[25] M. Tyloo, R. Delabays, and P. Jacquod, Phys. Rev. E **99**, 062213 (2019).

[26] J. Hindes and I. B. Schwartz, Chaos **28**, 071106 (2018).

[27] I. Z. Kiss, Y. Zhai, and J. L. Hudson, Phys. Rev. Lett. **94**, 248301 (2005).

[28] R. K. Niyogi and L. Q. English, Phys. Rev. E **80**, 066213 (2009).

[29] P. Ashwin and J. Borresen, Phys. Rev. E **70**, 026203 (2004).

[30] J. Lorenz, Int. J. Mod. Phys. C **18**, 1819 (2007).